

## Original Article

# The iron chelator Dp44mT suppresses osteosarcoma's proliferation, invasion and migration: in vitro and in vivo

Pengcheng Li<sup>1</sup>, Xun Zheng<sup>1</sup>, Kangquan Shou<sup>1,2</sup>, Yahui Niu<sup>1</sup>, Chao Jian<sup>1,3</sup>, Yong Zhao<sup>1</sup>, Wanrong Yi<sup>1</sup>, Xiang Hu<sup>1</sup>, Aixi Yu<sup>1</sup>

<sup>1</sup>Department of Orthopedics, Zhongnan Hospital of Wuhan University, Wuhan 430071, Hubei, China; <sup>2</sup>Molecular Imaging Program at Stanford, Canary Center at Stanford for Cancer Early Detection, Department of Radiology and Bio-X Program, Stanford University, Stanford, CA, USA; <sup>3</sup>Department of Biochemistry & Molecular Medicine, UC Davis School of Medicine, Sacramento 95871, CA, USA

Received September 24, 2016; Accepted December 8, 2016; Epub December 15, 2016; Published December 30, 2016

**Abstract:** Di-2-pyridylketone-4,4-dimethyl-3-thiosemicarbazone (Dp44mT), the novel iron chelator, has been reported to inhibit the tumorigenesis and progression of various cancer cells, including neuroblastoma, neuroepithelioma and prostate cancer. However, whether Dp44mT has anticancer effects in osteosarcoma is still unknown. Here, we investigated the antitumor action of Dp44mT in osteosarcoma and its underlying mechanisms. A human osteosarcoma 143B cell line *in vitro* and 143B xenograft in nude mice *in vivo* were utilized, the anticancer effects of Dp44mT were examined through methods of MTT assay, transwell, wound healing assay, flow cytometry, western blot, immunohistochemistry and H&E staining. We showed that Dp44mT inhibits cell proliferation, invasion and migration *in vitro*. In addition, flow cytometry further illustrated that Dp44mT suppression of 143B cell proliferation, invasion and migration were partially due to induction of cell apoptosis, cell cycle arrest in S phase and ROS production. Also *in vitro* and *in vivo*, the expression levels of Bcl2, Bax, Caspase3, Caspase9, LC3-II,  $\beta$ -catenin and its downstream targets such as C-myc and Cyclin D1 demonstrated that cell apoptosis and autophagy, as well as Wnt/ $\beta$ -catenin pathway were involved in Dp44mT induced osteosarcoma suppression. The Dp44mT inhibition of osteosarcoma was further verified via animal models. The findings indicated that *in vivo* Dp44mT showed a significant reduction in the 143B xenograft tumor growth and metastasis. In conclusion, our data demonstrated that Dp44mT has effective anticancer capability in osteosarcoma and that may represent a promising treatment strategy for osteosarcoma.

**Keywords:** Dp44mT, proliferation, invasion, migration, osteosarcoma

## Introduction

Osteosarcoma (OS) is a primary high-grade malignant bone neoplasm, affecting mostly children, adolescent and young adults [1-3]. It is the leading cause of cancer-relevant death in children worldwide [4]. Despite following the modern treatment regimens, the patients with metastasized OS have just achieved approximately 15% [5] of 5-year postoperative survival rate. This greatly poor prognosis of OS patients is largely associated with its high lung metastasis tendency [6, 7]. However, the identified molecular mechanism underlying OS progression and metastasis remains unclear. Therefore, it is essential to identify the molecular markers and the novel chemotherapeutic agents, which would give a new approach to manage the progression and metastasis of OS.

Iron (Fe) is the essential micronutrient for life. Fe-containing proteins play the critical role in energy metabolism, DNA synthesis and cell growth [8]. For cancer cells, their Fe requirements perform much more increased than their counterparts, normal cells, which can be proved by their significantly higher elevated level of the transferrin receptor 1 and enhanced uptake of iron [9]. Studies show that Fe deprivation can effectively suppress growth of the neoplastic cells and many iron chelators have been proved with the sensitive antitumor capacity, such as desferrioxamine (DFO) and 311 [10]. Therefore, these results suggest that Fe deprivation may be a great therapeutic strategy for preventing cancer progression and further investigation of the underlying molecular mechanisms of iron-chelator-based treatment regime can definitely lead to a deeper understanding of OS progression and metastasis.

Interestingly, iron chelators have historically been used to study the treatment of cancers because of their distinct and selective anticancer activity [11, 12]. It is unclear, however, what the precise molecular targets and mechanisms directly involved in. Currently, DFO is widespread used clinically for iron overload disease (e.g.  $\beta$ -thalassemia), whereas, as the first commercially available antitumor agent, its mild membrane permeability and short half-life period make it itself suffers serious limitations on antiproliferative activity. On the contrary, Dp44mT with more effective Fe-binding ligands and marked membrane permeability, shows tremendous potential to against neoplasm. Dp44mT is one of a new compound of di-2-pyridylketone thiosemicarbazone (DpT) group, which is particularly selectivity and affinity for Fe (III) [13]. This group of thiosemicarbazones has been demonstrated to suppress the epithelial-to-mesenchymal transition [14], as well as induce autophagy [15] and apoptosis [16] in different cancer cells. Unlike DFO, the redox-active iron complexes of Dp44mT in lysosomes play vital roles in its cytotoxic activity [17, 18]. In fact, Dp44mT generates reactive oxygen species (ROS) due to the redox-active iron complexes and result in enhancing lysosomal membrane permeability and cell death [19]. However, the effect of Dp44mT in OS has not been reported until now, so this study can lead to a further comprehending and therapy of OS.

The Wnt/ $\beta$ -catenin pathway plays a key role in OS progression and metastasis [20].  $\beta$ -catenin that regulates the expression of pivotal genes, and acts as a key intracellular signal transducer between cytoplasm and cytoplasm [21]. In addition,  $\beta$ -catenin participates in the coordination of cell cycle [22] and the dysregulation of  $\beta$ -catenin in nucleus can activate oncogenes [23-25]. Besides that, autophagy and apoptosis are two important catabolic pathways in cellular processes and determining cellular fate, one is the prosurvival pathway and other is the cell death pathway [26], a mass of studies [27-30] have been proved that in many cancers, the level of cell autophagy and apoptosis are greatly aberrant expression. Therefore, it is well worth finding what role these processes could play in the OS.

In the present study, we illustrate that Dp44mT suppresses OS growth and metastasis *in vitro* and *in vivo*. Moreover, we reveal that Dp44mT

significantly elevates autophagy and apoptosis flux, induces ROS production, arrests cell cycle in S phase and depresses Wnt/ $\beta$ -catenin pathway. These investigations suggest that Dp44mT could be a potential candidate for the treatment of OS.

### Materials and methods

#### *Cell culture and cell treatment*

Human OS cell line, 143B was obtained from CCTCC (China Center For Type Culture Collection). All cells were cultured in DMEM medium with 10% fetal bovine serum (Sigma, USA) and supplemented with 100 IU/mL penicillin (Gibco) and 100  $\mu$ g/mL streptomycin (Gibco) and incubated in a humidified incubator at 37°C with 5% CO<sub>2</sub> atmosphere. Dp44mT was purchased from Sigma. In this investigation, the chelator Dp44mT was utilized at concentration of 10  $\mu$ M since previous study [31] had proved that this low concentration demonstrated prominent iron chelation efficacy and marked membrane permeability, as well as showed significant time-dependent manner in our results. Dp44mT was dissolved in DMSO (Sigma) and diluted in medium (final concentration  $\leq$  0.1% (v/v)).

#### *MTT assay for cell proliferation*

Cells were seeded in 96-well plate at  $3.0 \times 10^3$  cells/well in 200  $\mu$ L of complete medium. After incubated for 24 hours at 37°C with 5% CO<sub>2</sub> humidified atmosphere, cells of each well was washed by phosphate buffered saline (PBS, pH=7.2, 10 mM) and then different concentration of Dp44mT (0.625 to 40  $\mu$ M) were added to each designed well (except to control well). After 24 hours, 48 hours and 72 hours, each well removed the Dp44mT solution, used PBS to wash and then added to MTT (5 mg/mL) solution, including the control well. After that, the mixture incubated 2 hours, then the MTT solution was replaced with 150  $\mu$ L of dimethyl sulfoxide (DMSO). Before measuring (the OD was measured at 490 nm), the 96-well plate was shaken at 37°C for 15 min.

#### *Detection of intracellular reactive oxygen species (ROS)*

The intracellular ROS level was measured by using the Reactive Oxygen Species Assay Kit (Beyotime, Nanjing, China). All experiment steps

## Dp44mT suppresses osteosarcoma

were following the manufacturer's instructions. Briefly, 143B cells pretreated with Dp44mT for 24 h, 48 h and 72 h, washed three times with DMEM serum-free medium. Then, DCFH-DA (10  $\mu$ mol) was added and incubated with cells in dark for 25 min at 37°C. After that, cells washed with PBS three times and detected the fluorescence by flow cytometry.

### *Analysis of cell cycle and apoptosis by flow cytometry*

Cells were harvested until 70-80% confluency was reached and then produced the single-cell suspension. 100  $\mu$ L of the RNase A solution and 100  $\mu$ L of the PI solution were added to the suspension and incubated for 30 min at room temperature (protection from light). Determination of cells in each phase of the cell cycle (G1, S, and G2 + M) used flow cytometry. The Annexin-FITC apoptosis detection kit was used to detect the cell apoptosis, all steps followed the manufacturer's protocols. The examination of samples used flow cytometry.

### *Wound healing assay*

Cells were plated onto dish to grow a 100% confluent layer. A p200 pipette tip was used to create a neat and straight line in the monolayer by scraping. The debris was removed by medium, and fresh medium with agent was added. Reference points were marked using a scalpel on the outer surface of the dish. The rate of cell migration in wound areas was determined at the 24 h and 48 h with the microscope and the images in each time point were captured (Magnification,  $\times 40$ ). Analysis and quantification of the healing rate used Image J Software. The wound-healing rate was calculated as following: (0 hour wound area -24 hour or 48 hour wound area)/0 hour wound area  $\times 100\%$ .

### *Transwell invasion assay*

Invasion of 143B cells was measured by using BD BioCoatt™ Invasion Chamber (Becton Dickinson Biosciences, USA). The two chambers were separated with 8- $\mu$ m pore size polycarbonate filters. The upper chamber was added to the Matrigel (BD Transduction Laboratories, USA) for 1 h at 37°C before use. 143B cells were first treated with 10  $\mu$ M of Dp44mT for 0 h, 24 h, 48 h and 72 h, respectively. Survived cells were collected and plated in the upper chamber at  $1.0 \times 10^5$  cells/well. The

complete (serum-containing) culture medium was placed in the lower chamber and then incubated at 37°C with 5% CO<sub>2</sub> for 24 h. After 24 h, the bottom side of the membrane were fixed with methanol for 20 min and stained with 0.1% gentian violet for 10 min. Invasive cells were counted and photographed at  $\times 200$  magnification under microscope.

### *Western blot analysis*

The whole cell protein lysates were extracted using ProteoJET™ Mammalian Cell Lysis Reagent (MBI Fermentas, Canada) supplemented with the complete protease inhibitors (Bestbio, China) according to the manufacturer's instructions. The protein concentration was determined using the Bradford protein assay kit (Beyotime Institute of Biotechnology). The total obtained proteins (40  $\mu$ g/lane) were separated on a 10% SDS-PAGE gel and transferred onto nitrocellulose membranes (Millipore, USA). The membranes were blocked in PBS, containing 5% skimmed milk and Tween-20 overnight at 4°C and then incubated with primary antibodies against Cyclin D1, Bcl2, Bax, Caspase3, Caspase9, LC3-I, LC3-II,  $\beta$ -catenin, C-myc and GAPDH, for 12 h at 4°C. Then the membranes were incubated with secondary antibodies labeled with horseradish peroxidase for 30 min at 4°C. Finally, the targeted bands were visualized with SuperSignal (Thermo Scientific, USA), GAPDH was used as a loading control.

### *Immunohistochemistry analysis*

Immunohistochemistry was performed with Bax antibody at a 1:200 dilution, Bcl2 antibody at a 1:400 dilution, C-myc antibody at a 1:400 dilution, Cyclin D1 antibody at a 1:100 dilution,  $\beta$ -catenin antibody at a 1:400 dilution and LC-3-II antibody at a 1:10 dilution. Briefly, tumor tissue sections were deparaffinized with xylene, and rehydrated through ethanol. The tissue sections were incubated with approximately 50  $\mu$ l dilute solution of primary antibody overnight at 4°C, followed by staining with secondary antibody for 50 min at 37°C. The slides were counterstained with heatoxylin, dehydrated in graded alcohols and mounted.

### *Tumor xenografts in nude mice*

*In vivo* experiments were approved by the Animal Ethics Committee (Zhongnan Hospital

of Wuhan University) and met the National Institutes of Health guidelines. In these studies, 6 week old male nude mice (BALBc nu/nu) were used and housed in SPF (specific-pathogen free) conditions, tumor xenografts were established by standard techniques [32]. Briefly, 143B cells were harvested until 80-90% confluency is reached and then suspended in PBS ( $5 \times 10^7$  cells/ml). 50  $\mu$ L of matrigel matrix (BD Biosciences, USA) were added to 50  $\mu$ L of PBS cell suspension. Then 100  $\mu$ L of the above mixture ( $2.5 \times 10^6$  cells) were injected subcutaneously into the flank of each nude mice, this area were then observed the tumor development daily. After engraftment, tumor size was measured by the caliper. Tumor volumes were calculated by the formula:  $(a \times b^2)/2$  (a: long axis and b: short axis of the tumor).

10 mice showing similar tumor sizes were selected and randomly divided into 2 group (Dp44mT vs Control, n=5), when tumor volumes reached 100 mm<sup>3</sup>, the nude mice were treated. In Dp44mT group, nude mice were treated with Dp44mT (0.4 mg/kg). Dp44mT was dissolved in 15% propylene glycol in 0.9% saline and intravenously injected (via tail vein) 5 days/week (Monday to Friday) [33]. In control group, nude mice were treated with vehicle alone (via tail vein). The growth curve of the tumor volume (mean  $\pm$  S.D.) in each group (n=5) was graphed. 30 days after injection, all animals were sacrificed and wet tumor weight in each group (n=5) was recorded before tumors were harvested.

### *Metastasis assay in nude mice*

The experiments were performed as described previously [34]. Briefly, a volume of 0.1 ml of cell suspension (143B cells,  $5 \times 10^7$  cells/ml PBS) was injected into the 10 nude mice via tail veins, then randomly divided into 2 groups (Dp44mT vs Control, n=5). The treatment measure was similar to the above nude mice experiments. Four weeks after injection, the nude mice were sacrificed. Lungs were dissected out and fixed in formaldehyde solution. Microscopic metastases were visualized on paraffin-embedded sections (5  $\mu$ m) after H&E staining. The number of lung sections containing tumor foci was counted.

### *Statistical analysis*

All data were performed using the SPSS 19.0 statistical software. Values were presented as

the mean  $\pm$  standard deviation (S.D.) and analyzed using one-way ANOVA or Student t-test. When then probability was less than 0.05 ( $P < 0.05$ ), the difference was considered as statistically significant. Each experiment was carried out at least three times.

## Results

### *Dp44mT suppressed cell proliferation*

The MTT assay was performed to determine the proliferation inhibitory effect of Dp44mT on human 143B OS cells. The data showed that Dp44mT significantly (**Figure 1A** and **1B**) suppressed the proliferation of 143B cells in different concentrations ( $P < 0.001$ ). Moreover, the inhibition rate indicated the significant time-dependent manner when the concentration of Dp44mT in 10  $\mu$ M and 20  $\mu$ M (**Figure 1B**). The results revealed that Dp44mT had the effective activity in reducing the proliferation of OS cells.

### *Dp44mT suppressed the migration and invasion of 143B cells*

The wound healing and transwell invasion assays were carried out to assess the effect of Dp44mT on cell migration and invasion of 143B cells, because these two characteristics of tumor cell play a pivotal role in the process of tumor progression and metastasis. In case of the cell proliferation rates influenced the migration and invasion capacity of 143B cells, the medium of both assays were without FBS. The data (**Figure 1C** and **1D**) showed that, compared with blank control (without Dp44mT) at 24 h and 48 h, Dp44mT (10  $\mu$ M) treatment group effectively reduced the wound-healing rate ( $12.64\% \pm 2.57\%$  vs  $42.54\% \pm 3.28\%$ ,  $35.02\% \pm 3.41\%$  vs  $79.38\% \pm 6.76\%$ ) of 143B cells line, respectively. The data of the transwell invasion assay illustrated that the invasive capacity of 143B cells were significantly inhibited after incubated with Dp44mT (10  $\mu$ M) at 24 h, 48 h and 72 h, respectively (**Figure 1E** and **1F**). These results demonstrated that Dp44mT distinctly attenuated the migration and invasion of 143B cell *in vitro*.

### *Dp44mT induced 143B cells apoptosis*

To investigate the mechanism underling Dp44mT induced anti-proliferation, we used the flow cytometric analyses to detect the apoptotic profiles of 143B cells. The data

## Dp44mT suppresses osteosarcoma

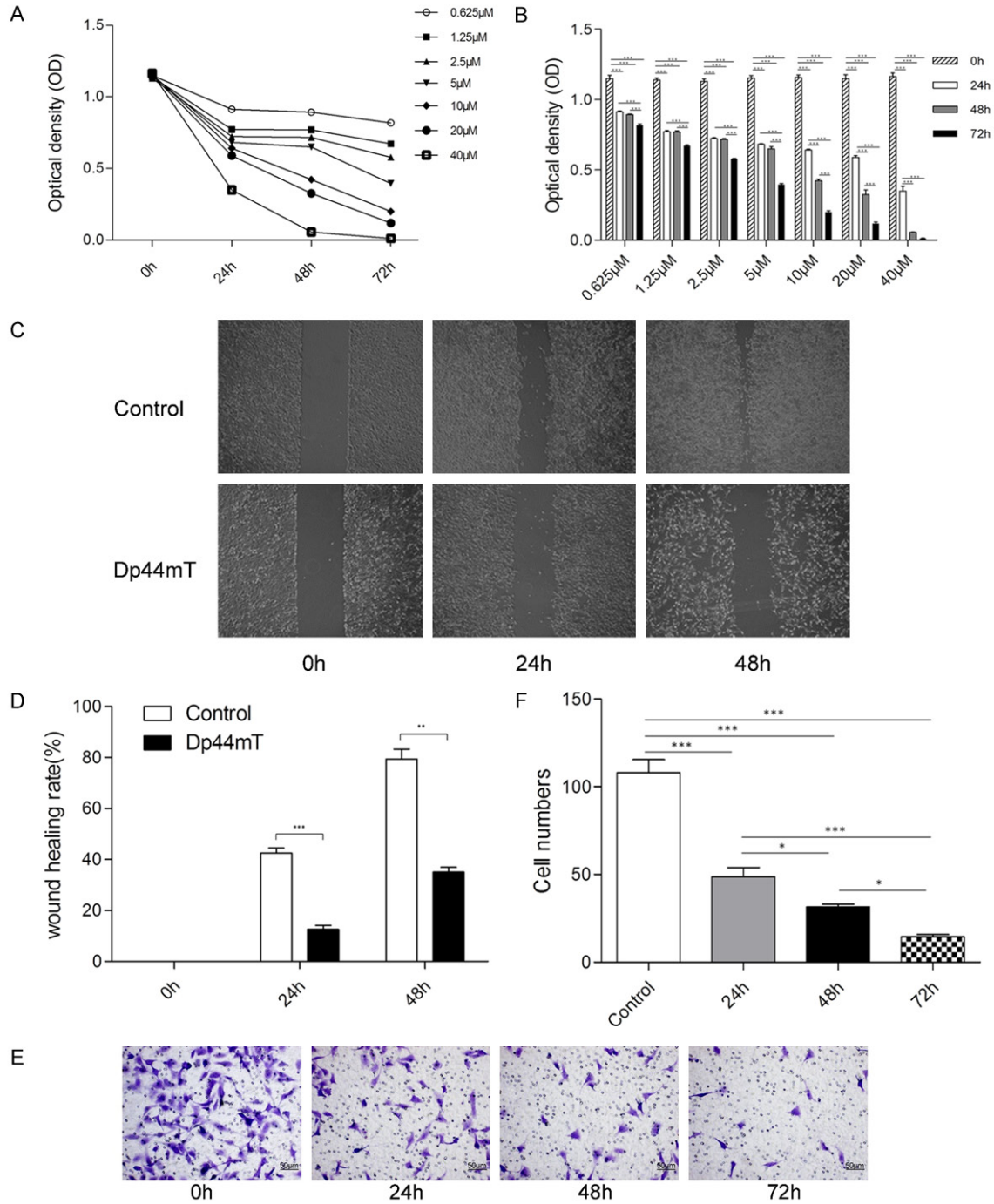
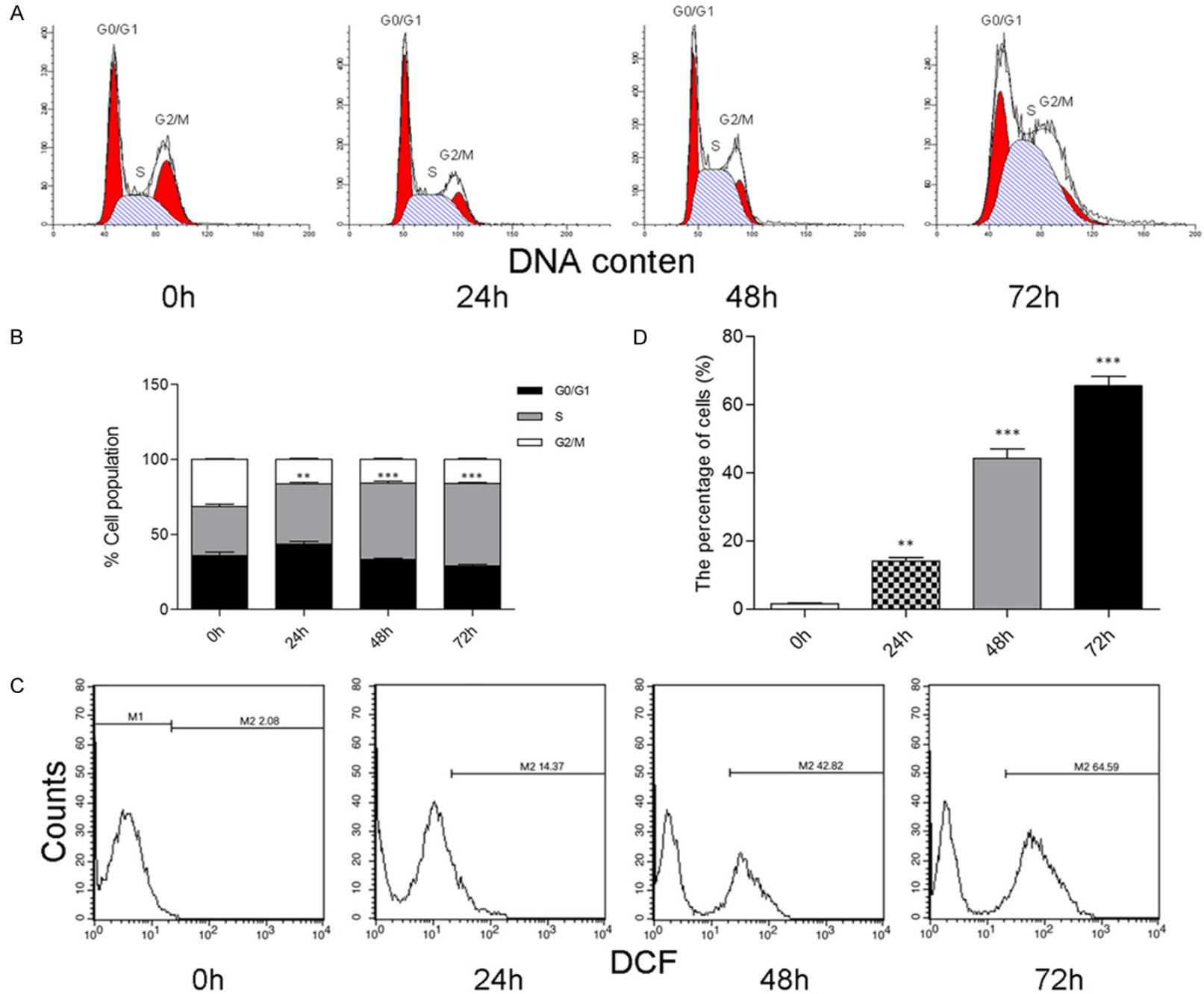


**Figure 1.** Dp44mT inhibits osteosarcoma cell proliferation, migration and invasion. A and B: MTT assay for the 143B cell line, 143B treated with Dp44mT at a range of concentrations (0.625 to 40 μM) for 0 h, 24 h, 48 h and 72 h. C: Wound healing assay for 143B cell line, 143B treated with Dp44mT (10 μM), the images were taken at 0 h, 24 h and 48 h (Magnification, ×40); D: The average area of the wound healing rate used Image J Software. E: Transwell invasion assay for 143B cell line, 143B treated with Dp44mT (10 μM) for 0 h, 24 h, 48 h, 72 h (Magnification, ×200); F: Invasion cell numbers after Dp44mT (10 μM) treatment. All results represent mean ± S.D. for three times independent experiments. Relative to control: \* $P < 0.05$ ; \*\* $P < 0.01$ ; \*\*\* $P < 0.001$ .

showed that Dp44mT (10 μM) strikingly increased the apoptotic cells in 143B cell line

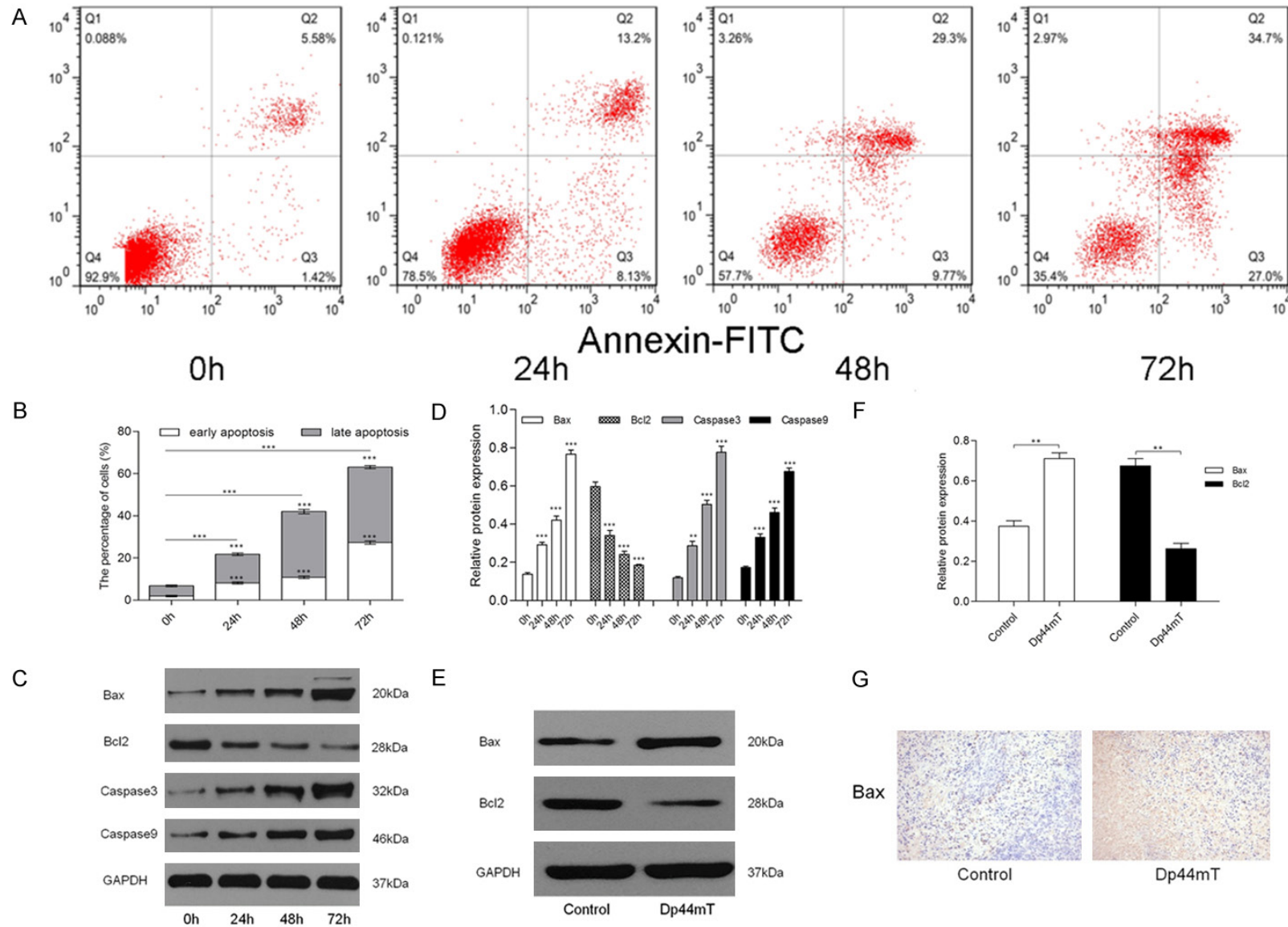
and following the distinct time-dependent manner (Figure 3A and 3B). The apoptotic rate of

Dp44mT suppresses osteosarcoma



## Dp44mT suppresses osteosarcoma

**Figure 2.** Dp44mT induces S population and ROS accumulation. Flow cytometry was used to detect the cell cycle and ROS. A and B: The S population of 143B was significantly increased after Dp44mT (10  $\mu$ M) treatment. C and D: As the time went on, Dp44mT (10  $\mu$ M) remarkably increased ROS level of 143B. All results represent mean  $\pm$  S.D. for three times independent experiments. Relative to control: \* $P < 0.05$ ; \*\* $P < 0.01$ ; \*\*\* $P < 0.001$ .



## Dp44mT suppresses osteosarcoma

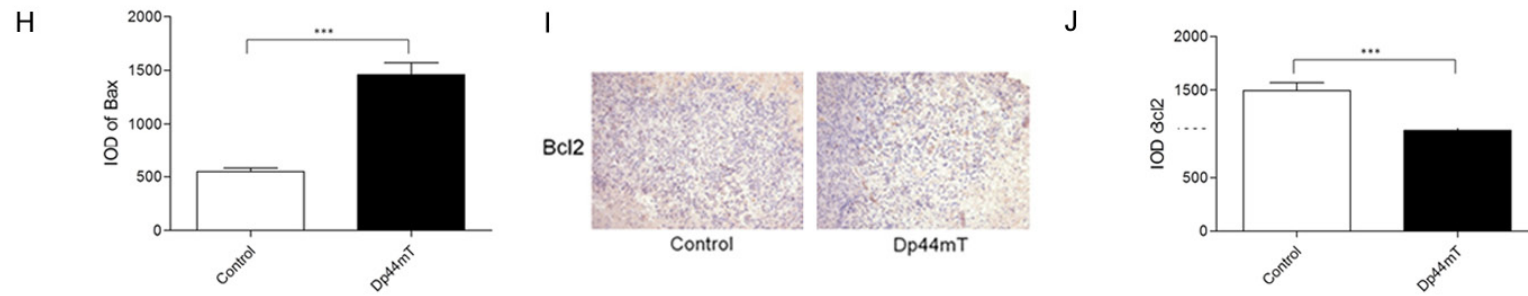


**Figure 3.** Dp44mT induces apoptosis *in vitro* and *in vivo*. A and B: *In vitro*, flow cytometry was used to detect the cell apoptosis, the results of apoptosis rate of 143B treated with Dp44mT (10  $\mu$ M) for 0 h, 24 h, 48 h and 72 h. C and D: *In vitro*, the expression of apoptosis-related proteins: Bax, Bcl-2, Caspase-3 and Caspase-9. E-J: *In vivo*, the expression of apoptosis-related proteins: Bax and Bcl-2. Immunohistochemistry (Magnification,  $\times 200$ ). All results represent mean  $\pm$  S.D. for three times independent experiments. Relative to control: \* $P < 0.05$ ; \*\* $P < 0.01$ ; \*\*\* $P < 0.001$ .

## Dp44mT suppresses osteosarcoma

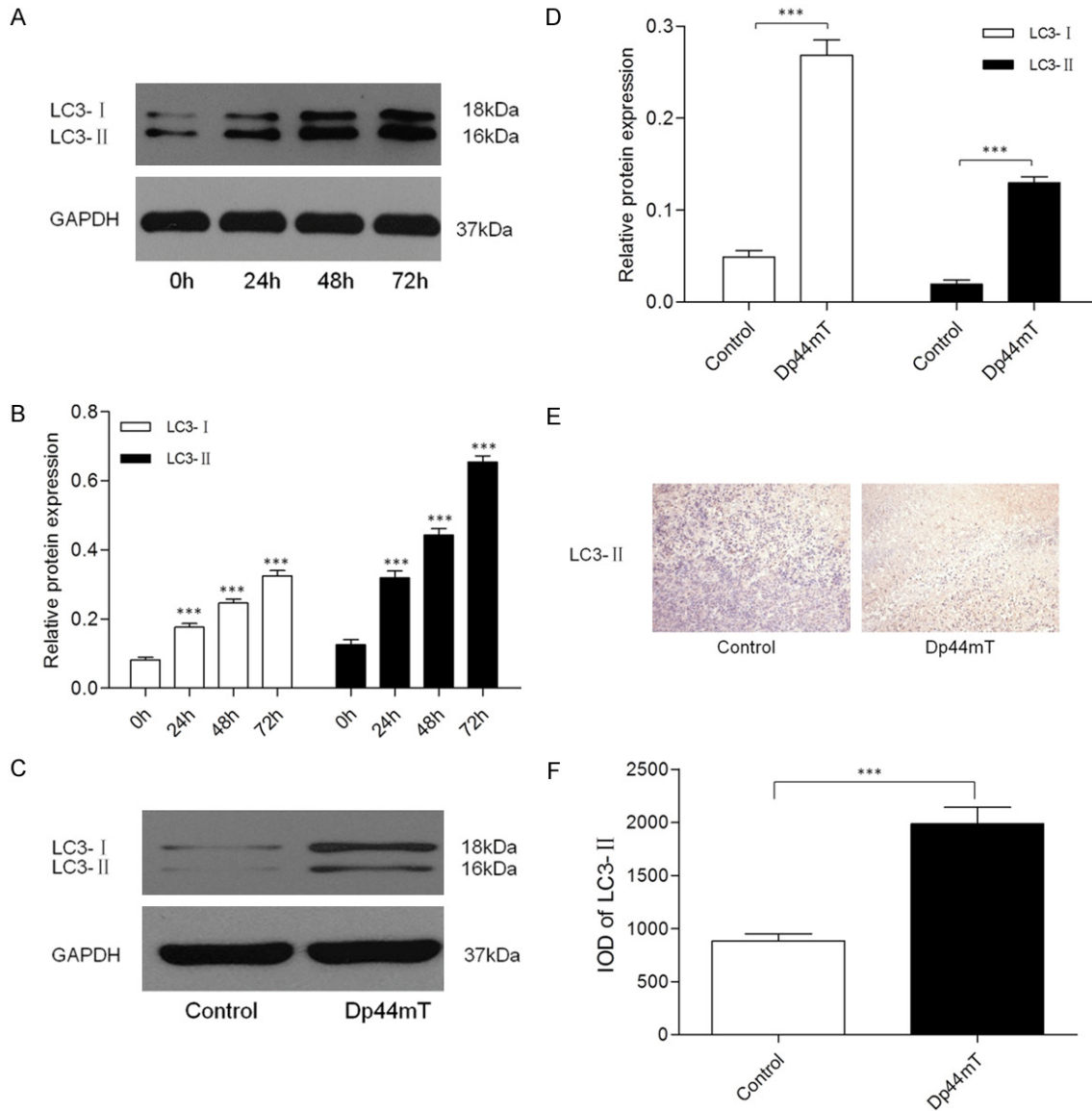


**Figure 4.** Dp44mT induces autophagy *in vitro* and *in vivo*. A and B: *In vitro*, the protein expression of the LC3-I and LC3-II. C-F: *In vivo*, the protein expression of the LC3-I and LC3-II. Immunohistochemistry (Magnification,  $\times 200$ ). All results represent mean  $\pm$  S.D. for three times independent experiments. Relative to control: \* $P < 0.05$ ; \*\* $P < 0.01$ ; \*\*\* $P < 0.001$ .

cells at 0 h, 24 h, 48 h and 72 h were  $6.78\% \pm 0.23\%$ ,  $21.76\% \pm 1.88\%$ ,  $42.00\% \pm 2.86\%$  and  $63.08\% \pm 2.5\%$  ( $P < 0.001$ ), respectively. Moreover, the Dp44mT (10  $\mu\text{M}$ ) induced the early apoptosis and the late apoptosis, respectively. Additionally, we used the western blot (Figure 3C and 3E) and immunohistochemistry (Figure 3G and 3I) to detect the apoptosis-related proteins, Bax and Bcl-2 level. The results demonstrated that Dp44mT (10  $\mu\text{M}$  or 0.4 mg/kg) can significantly increase proapoptotic Bax protein and decrease anti-apoptotic Bcl-2 protein level when compared with blank

control. Moreover, the Caspase-3 and Caspase-9 activity revealed the same tendency (Figure 3C and 3D), markedly increased, in Dp44mT (10  $\mu\text{M}$ ) treatment groups at each time point. These results showed that Dp44mT induced the proliferation inhibitory effect via the apoptotic pathway.

### Dp44mT induced 143B cells S phase arrest

To assess how Dp44mT affects the cell cycle progression of the OS cell line, cells were stained with propidium iodide (PI) and analyzed

## Dp44mT suppresses osteosarcoma

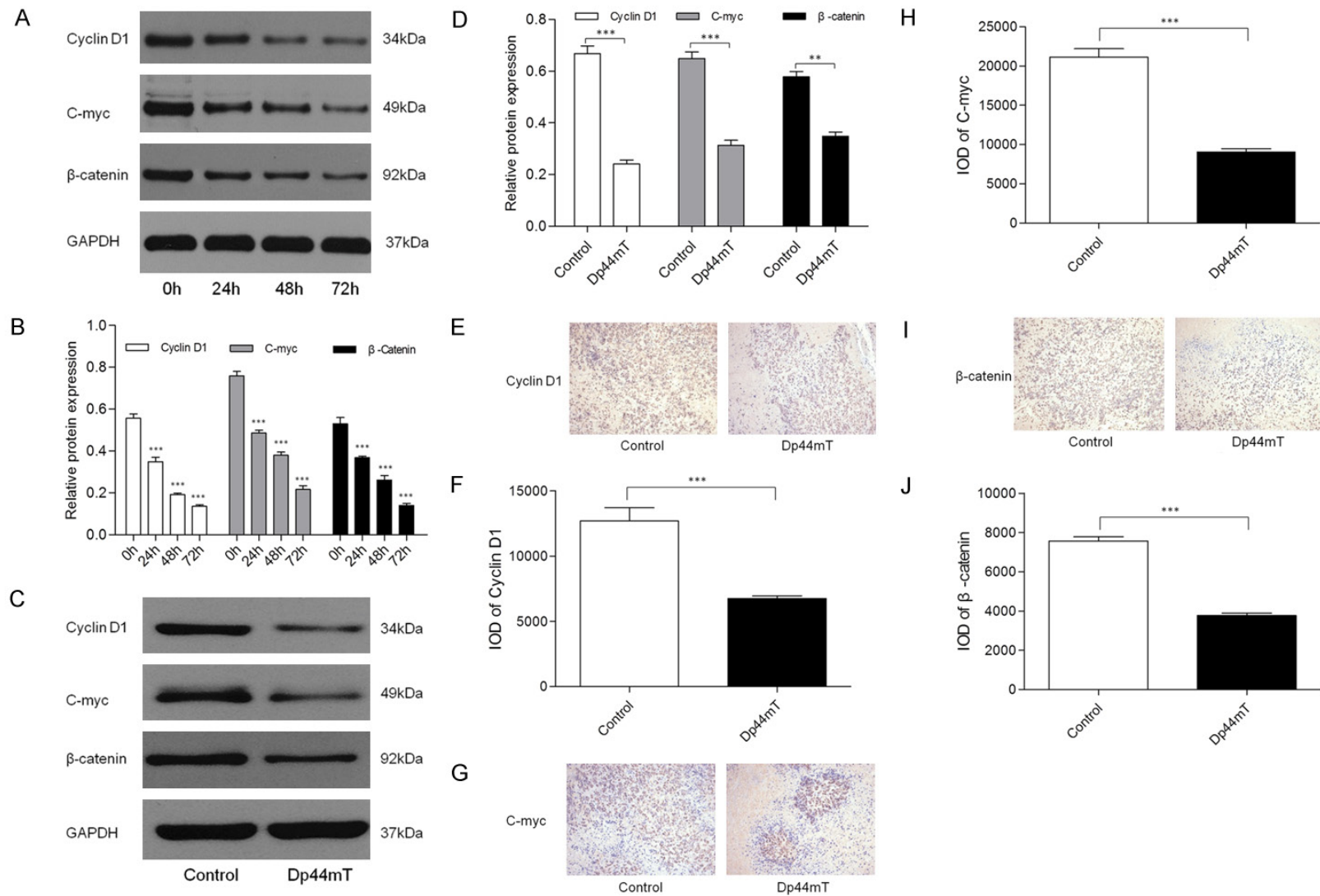


**Figure 5.** Dp44mT inhibits the Wnt/ $\beta$ -catenin signaling pathway *in vitro* and *in vivo*. A and B: *In vitro*, the protein expression of Wnt/ $\beta$ -catenin canonical signaling,  $\beta$ -catenin and its downstream genes, c-Myc and cyclin D1. C-J: *In vivo*, the protein expression of Wnt/ $\beta$ -catenin canonical signaling,  $\beta$ -catenin and its downstream genes, c-Myc and cyclin D1. Immunohistochemistry (Magnification,  $\times 200$ ). All results represent mean  $\pm$  S.D. for three times independent experiments. Relative to control: \* $P < 0.05$ ; \*\* $P < 0.01$ ; \*\*\* $P < 0.001$ .

## Dp44mT suppresses osteosarcoma

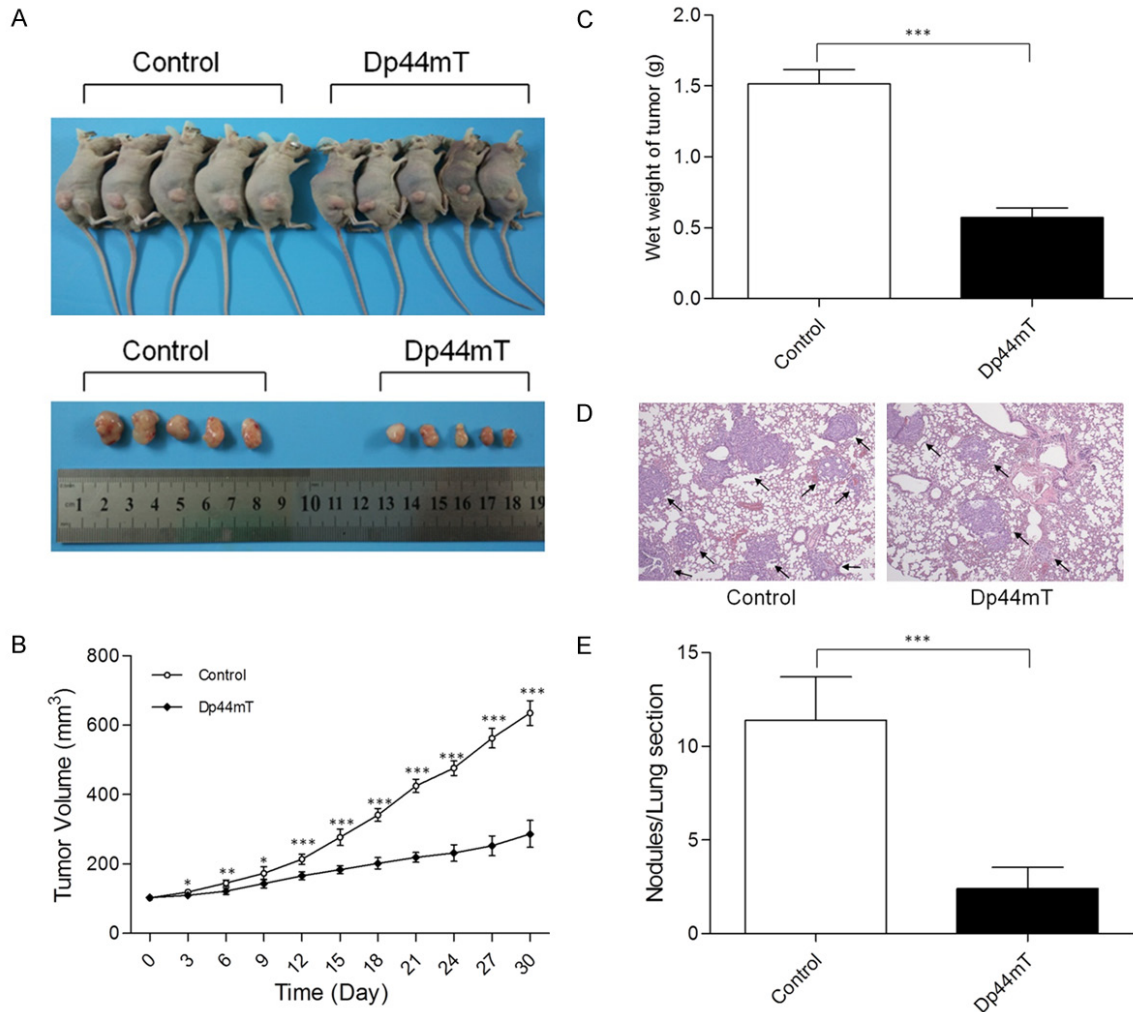


**Figure 6.** Dp44mT suppresses lung tumor growth and metastasis in nude mice. A: Tumor bearing nude mice (n=5) and the tumor tissues (n=5). B: Tumor growth curve which was graphed by the mean tumor volume (n=5). C: Average tumor wet weight in each group (n=5) was recorded after nude mice were sacrificed. D: Images of lung sections by H&E staining (Magnification,  $\times 40$ ). Arrows represent lung metastatic nodules. E: The mean number of lung nodules per section in each group (n=5). All results represent mean  $\pm$  S.D. for three times independent experiments. Relative to control: \* $P < 0.05$ ; \*\* $P < 0.01$ ; \*\*\* $P < 0.001$ .

by flow cytometry at 0 h, 24 h, 48 h and 72 h, respectively. The results showed that Dp44mT (10  $\mu$ M) markedly led to 143B cells accumulated in S phase ( $P < 0.01$ ) in a time-dependent manner (Figure 2A and 2B), illustrating that Dp44mT arrested the cell cycle at S phase in 143B cells, which was associated with its anti-proliferation function.

### Dp44mT induced the ROS accumulation and autophagy

Previously it was suggested that Dp44mT induced reactive oxygen species (ROS) accumulation [35-37], which increased cytotoxicity.

To prove that, we performed the experiments to examine the total ROS production after 143B cells incubated with Dp44mT (10  $\mu$ M). Figure 2C showed that there was strikingly difference in the ROS levels in the 143B cells for 0 h, 24 h, 48 h and 72 h ( $P < 0.01$ ), respectively, and the longer incubation the stronger ROS production.

Considering that Dp44mT can deplete cellular iron and induce autophagy, which is vital to cell survival, and the transformation of LC3-I to LC3-II is an essential step to form the autophagosome. Therefore, the experiments were performed to investigate the proteins expression

of the LC3-I and LC3-II *in vivo* and *in vitro*. Interestingly, the data showed that with the 143B cells were incubated with Dp44mT (10  $\mu$ M) for 0 h, 24 h, 48 h and 72 h, protein level of LC3-I and LC3-II significantly increased (**Figure 4A**). Besides that, the results of the LC3-I and LC3-II protein level in tumor xenografts with the Dp44mT (0.4 mg/kg) treatment displayed the similar trend (**Figure 4C** and **4E**). These results indicated that Dp44mT could increase autophagy to response the stress induced by iron depletion.

### *Dp44mT inhibited the Wnt/ $\beta$ -catenin signaling pathway*

The OS cell lines are regulated by various essential signaling pathways, the Wnt/ $\beta$ -catenin canonical pathway is included. In this study, we evaluated whether Dp44mT could have an effect on the Wnt/ $\beta$ -catenin canonical signaling and the expression of its downstream genes, C-myc and Cyclin D1. In human OS cell line 143B and tumor tissue, we set out to examine  $\beta$ -catenin, C-myc and Cyclin D1 expression levels for different time of Dp44mT through western blot and immunohistochemistry (**Figure 5**). The data showed that with the treatment of Dp44mT (10  $\mu$ M or 0.4 mg/kg), these proteins expression level significantly decreased. These results demonstrated that Dp44mT promoted the degradation of  $\beta$ -catenin and then reduced the expression of its downstream genes, C-myc and Cyclin D1.

### *Dp44mT suppressed lung tumor growth and metastasis in vivo*

To validate the anti-tumor growth effects of Dp44mT *in vivo*, we performed subcutaneous xenograft of 143B cells into nude mice. All animals were sacrificed after 30 days, the size and wet weight of tumors in each group (n=5) was recorded. In these findings, the nude mice in Dp44mT (0.4 mg/kg) group demonstrated a strikingly slower growth rate than control group (**Figure 6A** and **6B**). In addition, **Figure 6C** showed that Dp44mT (0.4 mg/kg) reduced about 62.22% average wet weight of tumors compared with control group.

To identify the effect of Dp44mT on metastasis of OS cells *in vivo*, nude mice were intravenously injected with 143B cells. The metastatic lung nodules were counted after 4 weeks. Quanti-

fication of the metastatic nodules that developed in the nude mice lungs indicated that Dp44mT (0.4 mg/kg) significantly inhibited the metastatic activity of 143B cells compared with control group (**Figure 6D** and **6E**). These experiments revealed that the Dp44mT was capable of inhibiting OS cells growth and metastasis *in vivo*, which corroborated well with the data that found *in vitro*.

## Discussion

OS is the most popular aggressive malignant bone sarcomas, which involves in rapid metastasizing behavior and therapy resistance. Recently, the treatment of OS via traditional surgical resection associates with radio-chemotherapy is less than satisfactory. However, emerging data suggest that iron chelators have been used as the new drug and achieve notable effect in many cancers treatment, from which Dp44mT is the most potent and selective one. A variety of studies [38, 39] have shown that as the novel anti-cancer agent, Dp44mT not only effectively suppressed the tumor growth but also strikingly decreased the distant metastasis. In this investigation, we demonstrated that Dp44mT's contribution to suppressing OS growth and metastasis. Additionally, we found that Dp44mT inhibited proliferation, invasion, migration and Wnt/ $\beta$ -catenin signaling pathway, as well as increased autophagy and apoptosis of OS *in vitro* in human OS cell line and *in vivo* using OS xenograft tumor mouse models. In conclusion, these results are meaningful for understanding the role of Dp44mT as the novel potential anticancer agent and may explore the new treatment and preventive strategy in OS.

Cell proliferation, migration and invasion capacity closely regulate the cancer generation and development, which are the pivotal parts of cancer metastasis. Hence, the influences of Dp44mT on these characteristics in 143B cells were further investigated. Wang J et al. [31] reported that hepatocellular carcinoma invasive property was significantly inhibited after Dp44mT treatment, and *in vivo* treatment, Dp44mT also remarkably decreased the number of lung metastatic nodules and the size of lung metastatic lesions. Besides that, Patric J. Jansson et al. [40] showed that Dp44mT markedly suppressed the subcutaneous human tumor xenograft. In agreement with that, our

present experiment demonstrated that, *in vitro*, the proliferation and migration rate of 143B (Figure 1A-D), as well as the cells invaded through the Matrigel (Figure 1E and 1F) were notably declined by Dp44mT application. Furthermore, *in vivo*, the average size, wet weight and lung metastatic nodules of the nude mice xenograft tumor were also potently inhibited by Dp44mT (Figure 6). Therefore, these results illustrate that as the anti-cancer reagent, Dp44mT contribute to the inhibition of proliferation, migration and invasion properties in OS.

Cell death, including apoptosis and autophagic cell death, is the critical and active process that maintains cell metabolism. Autophagy is a pro-survival mechanism, nevertheless, there are several evidences of autophagic cell death demonstrated that it promotes cell death. Occurrence of autophagic cell death can accompany by apoptosis or act as the complementary mechanism when apoptosis is insufficient [41, 42]. Besides that, some anti-proliferation drugs can enhance autophagic cell death process when cells apoptosis pathway is defective [43, 44]. Previous studies have reported that Dp44mT inhibited various cancers by inducing apoptosis, autophagy and cell cycle arrest. Similarly, in this study, Dp44mT induced both early and late apoptosis (Figure 3A and 3B), moreover, Dp44mT provoked much greater levels of late apoptosis and S cell cycle arrest (Figure 2A and 2B), which was consistent with the dramatic effects in inhibiting 143B cell progression. Furthermore, we investigated the degrees of the pro-apoptotic protein, Bax and anti-apoptotic protein, Bcl-2 as well as caspase-3 and caspase-9 (Figure 3C-J). After a 0 h, 24 h, 48 h and 72 h incubation with Dp44mT, Bax, caspase-3 and caspase-9 expression remarkably increased and Bcl-2 notably declined, in accordance with its previous report. As our expectation, the protein expression of autophagy marker LC3-II significantly increased and the similar results were found for LC3-I, slight but significant (Figure 4A-D). To interpret the possible mechanism in which Dp44mT enhanced autophagy, the degrees of ROS were analyzed, the data revealed that Dp44mT strikingly increased the ROS level of 143B (Figure 2C and 2D). It is known that Dp44mT can deprive cellular iron to produce cytotoxic redox-active complexes, which induces cytotoxic ROS [45]. However, as the cytoprotective process, auto-

phagy is always accompanied by ROS production [46]. Previous study has found that lysosome is ROS classical target, which leads to the destabilization of lysosomal membrane and then results in cellular damage [47]. Therefore, once the normal balance between ROS production and degradation are disturbed, the hydrolytic enzymes are released from destabilization lysosomal membrane, which may be the key mechanism of Dp44mT inducing autophagy and then promoting cell death.

Alteration of Wnt/ $\beta$ -catenin signaling has been identified in many kinds of carcinoma and found to be associated with cancer progression [48-50].  $\beta$ -catenin, the most critical members of this canonical pathway, exerts key function to activate specific biological effect. Therefore, in the present study, we analyzed the expression levels of  $\beta$ -catenin in 143B cell line (Figure 5A, 5C and 5I), the data revealed that  $\beta$ -catenin protein expression was significantly reduced, which made its downstream targets genes, C-myc and Cyclin D1, perform the similar down-regulated trend (Figure 5A, 5C, 5E and 5G). Accordingly, these results suggest that Wnt/ $\beta$ -catenin signaling can involve in the mechanism of Dp44mT to exert the anti-tumor capability, in which  $\beta$ -catenin plays the essential effect.

In conclusion, this study has identified Dp44mT, a potent anti-cancer agent, mediates multiple facets important to OS development and metastasis. In particular, the data demonstrate that Dp44mT significantly inhibits proliferation, invasion and migration of osteosarcoma *in vitro* and *in vivo*.

### Acknowledgements

The authors thank the fund support from Aixi Yu's Outstanding Medical Academic Leader Program of Hubei Province.

### Disclosure of conflict of interest

None.

**Address correspondence to:** Drs. Xiang Hu and Aixi Yu, Department of Orthopedics, Zhongnan Hospital of Wuhan University, No. 169, Donghu Road, Wuhan 430071, Hubei, China. Tel: +86 159 2623 8187; Fax: +86 27 6875 8696; E-mail: shawnhu2011@163.com (XH); Tel: +86 135 0718 7489; Fax: +86 27 6875 8696; E-mail: yuaixi@whu.edu.cn (AXY)

## References

- [1] Gorlick R, Janeway K, Lessnick S, Randall RL and Marina N. Children's oncology group's 2013 blueprint for research: bone tumors. *Pediatr Blood Cancer* 2013; 60: 1009-1015.
- [2] Rivera-Valentin RK, Zhu L and Hughes DP. Bone sarcomas in pediatrics: progress in our understanding of tumor biology and implications for therapy. *Paediatr Drugs* 2015; 17: 257-271.
- [3] Isakoff MS, Bielack SS, Meltzer P and Gorlick R. Osteosarcoma: current treatment and a collaborative pathway to success. *J Clin Oncol* 2015; 33: 3029-3035.
- [4] Botter SM, Neri D and Fuchs B. Recent advances in osteosarcoma. *Curr Opin Pharmacol* 2014; 16: 15-23.
- [5] Ma Y, Zhu B, Liu X, Yu H, Yong L, Liu X, Shao J and Liu Z. Inhibition of oleandrin on the proliferation and invasion of osteosarcoma cells in vitro by suppressing wnt/beta-catenin signaling pathway. *J Exp Clin Cancer Res* 2015; 34: 115.
- [6] Brennecke P, Arlt MJ, Campanile C, Husmann K, Gvozdenovic A, Apuzzo T, Thelen M, Born W and Fuchs B. CXCR4 antibody treatment suppresses metastatic spread to the lung of intratibial human osteosarcoma xenografts in mice. *Clin Exp Metastasis* 2014; 31: 339-349.
- [7] Luetke A, Meyers PA, Lewis I and Juergens H. Osteosarcoma treatment-where do we stand? A state of the art review. *Cancer Treat Rev* 2014; 40: 523-532.
- [8] Le NT and Richardson DR. The role of iron in cell cycle progression and the proliferation of neoplastic cells. *Biochim Biophys Acta* 2002; 1603: 31-46.
- [9] Raza M, Chakraborty S, Choudhury M, Ghosh PC and Nag A. Cellular iron homeostasis and therapeutic implications of iron chelators in cancer. *Curr Pharm Biotechnol* 2014; 15: 1125-1140.
- [10] Marques O, Da Silva BM, Porto G and Lopes C. Iron homeostasis in breast cancer. *Cancer Lett* 2014; 347: 1-14.
- [11] Corce V, Gouin SG, Renaud S, Gaboriau F and Deniaud D. Recent advances in cancer treatment by iron chelators. *Bioorg Med Chem Lett* 2016; 26: 251-256.
- [12] Yu Y, Gutierrez E, Kovacevic Z, Saletta F, Obeidy P, Suryo RY and Richardson DR. Iron chelators for the treatment of cancer. *Curr Med Chem* 2012; 19: 2689-2702.
- [13] Myers JM, Cheng Q, Antholine WE, Kalyanaraman B, Filipovska A, Arner ESJ and Myers CR. Redox activation of Fe(III)-thiosemicarbazones and Fe(III)-bleomycin by thioredoxin reductase: specificity of enzymatic redox centers and analysis of reactive species formation by ESR spin trapping. *Free Radic Biol Med* 2013; 60: 183-194.
- [14] Chen Z, Zhang D, Yue F, Zheng M, Kovacevic Z and Richardson DR. The iron chelators Dp44mT and DFO inhibit TGF-beta-induced epithelial-mesenchymal transition via up-regulation of N-Myc downstream-regulated gene 1 (NDRG1). *J Biol Chem* 2012; 287: 17016-17028.
- [15] Sahni S, Bae DH, Lane DJ, Kovacevic Z, Kalinowski DS, Jansson PJ and Richardson DR. The metastasis suppressor, N-myc downstream-regulated gene 1 (NDRG1), inhibits stress-induced autophagy in cancer cells. *J Biol Chem* 2014; 289: 9692-9709.
- [16] Noolsri E, Richardson DR, Lerdwana S, Fucharoen S, Yamagishi T, Kalinowski DS and Pattanapanyasat K. Antitumor activity and mechanism of action of the iron chelator, Dp44mT, against leukemic cells. *Am J Hematol* 2009; 84: 170-176.
- [17] Lovejoy DB, Sharp DM, Seebacher N, Obeidy P, Prichard T, Stefani C, Basha MT, Sharpe PC, Jansson PJ, Kalinowski DS, Bernhardt PV and Richardson DR. Novel second-generation di-2-pyridylketone thiosemicarbazones show synergism with standard chemotherapeutics and demonstrate potent activity against lung cancer xenografts after oral and intravenous administration in vivo. *J Med Chem* 2012; 55: 7230-7244.
- [18] Gaal A, Orgovan G, Polgari Z, Reti A, Mihucz VG, Bosze S, Szoboszlai N and Strelci C. Complex forming competition and in-vitro toxicity studies on the applicability of di-2-pyridylketone-4,4-dimethyl-3-thiosemicarbazone (Dp44mT) as a metal chelator. *J Inorg Biochem* 2014; 130: 52-58.
- [19] Gutierrez E, Richardson DR and Jansson PJ. The Anticancer Agent Di-2-pyridylketone 4,4-Dimethyl-3-thiosemicarbazone (Dp44mT) overcomes prosurvival autophagy by two mechanisms: persistent induction of autophagosome synthesis and impairment of lysosomal integrity. *J Biol Chem* 2014; 289: 33568-33589.
- [20] Tian J, He H and Lei G. Wnt/beta-catenin pathway in bone cancers. *Tumour Biol* 2014; 35: 9439-9445.
- [21] Lin CH, Ji T, Chen CF and Hoang BH. Wnt signaling in osteosarcoma. *Adv Exp Med Biol* 2014; 804: 33-45.
- [22] Li J, Yang S, Su N, Wang Y, Yu J, Qiu H and He X. Overexpression of long non-coding RNA HOTAIR leads to chemoresistance by activating the Wnt/beta-catenin pathway in human ovarian cancer. *Tumour Biol* 2016; 37: 2057-2065.
- [23] Nagaraj AB, Joseph P, Kovalenko O, Singh S, Armstrong A, Redline R, Resnick K, Zanotti K,

## Dp44mT suppresses osteosarcoma

- Waggoner S and DiFeo A. Critical role of wnt/beta-catenin signaling in driving epithelial ovarian cancer platinum resistance. *Oncotarget* 2015; 6: 23720-23734.
- [24] Chen EY, DeRan MT, Ignatius MS, Grandinetti KB, Clagg R, McCarthy KM, Lobbaridi RM, Brockmann J, Keller C, Wu X and Langenau DM. Glycogen synthase kinase 3 inhibitors induce the canonical wnt/beta-catenin pathway to suppress growth and self-renewal in embryonal rhabdomyosarcoma. *Proc Natl Acad Sci U S A* 2014; 111: 5349-5354.
- [25] Xue M, Wang Q, Zhao J, Dong L, Ge Y, Hou L, Liu Y and Zheng Z. Docosaheptaenoic acid inhibited the wnt/beta-catenin pathway and suppressed breast cancer cells in vitro and in vivo. *J Nutr Biochem* 2014; 25: 104-110.
- [26] Su M, Mei Y and Sinha S. Role of the crosstalk between autophagy and apoptosis in cancer. *J Oncol* 2013; 2013: 102735.
- [27] Arlt A, Muerkoster SS and Schafer H. Targeting apoptosis pathways in pancreatic cancer. *Cancer Lett* 2013; 332: 346-358.
- [28] Hassan M, Watari H, AbuAlmaaty A, Ohba Y and Sakuragi N. Apoptosis and molecular targeting therapy in cancer. *Biomed Res Int* 2014; 2014: 150845.
- [29] Galluzzi L, Pietrocola F, Bravo-San PJ, Amara-vadi RK, Baehrecke EH, Cecconi F, Codogno P, Debnath J, Gewirtz DA, Karantza V, Kimmelman A, Kumar S, Levine B, Maiuri MC, Martin SJ, Penninger J, Piacentini M, Rubinsztein DC, Simon HU, Simonsen A, Thorburn AM, Velasco G, Ryan KM and Kroemer G. Autophagy in malignant transformation and cancer progression. *EMBO J* 2015; 34: 856-880.
- [30] Jiang X, Overholtzer M and Thompson CB. Autophagy in cellular metabolism and cancer. *J Clin Invest* 2015; 125: 47-54.
- [31] Wang J, Yin D, Xie C, Zheng T, Liang Y, Hong X, Lu Z, Song X, Song R, Yang H, Sun B, Bhatta N, Meng X, Pan S, Jiang H and Liu L. The iron chelator Dp44mT inhibits hepatocellular carcinoma metastasis via N-Myc downstream-regulated gene 2 (NDRG2)/gp130/STAT3 pathway. *Oncotarget* 2014; 5: 8478-8491.
- [32] Kovacevic Z, Chikhani S, Lui GY, Sivagurunathan S and Richardson DR. The iron-regulated metastasis suppressor NDRG1 targets NEDD4L, PTEN, and SMAD4 and Inhibits the PI3K and Ras signaling pathways. *Antioxid Redox Sign* 2013; 18: 874-887.
- [33] Whitnall M, Howard J, Ponka P and Richardson DR. A class of iron chelators with a wide spectrum of potent antitumor activity that overcomes resistance to chemotherapeutics. *Proc Natl Acad Sci U S A* 2006; 103: 14901-14906.
- [34] Liu XH, Liu ZL, Sun M, Liu J, Wang ZX and De W. The long non-coding RNA HOTAIR indicates a poor prognosis and promotes metastasis in non-small cell lung cancer. *BMC Cancer* 2013; 13: 464.
- [35] Lovejoy DB, Jansson PJ, Brunk UT, Wong J, Ponka P and Richardson DR. Antitumor activity of metal-chelating compound Dp44mT is mediated by formation of a redox-active copper complex that accumulates in lysosomes. *Cancer Res* 2011; 71: 5871-5880.
- [36] Richardson DR, Sharpe PC, Lovejoy DB, Senaratne D, Kalinowski DS, Islam M and Bernhardt PV. Dipyriddy thiosemicarbazone chelators with potent and selective antitumor activity form iron complexes with redox activity. *J Med Chem* 2006; 49: 6510-6521.
- [37] Yuan J, Lovejoy DB and Richardson DR. Novel di-2-pyridyl-derived iron chelators with marked and selective antitumor activity: in vitro and in vivo assessment. *Blood* 2004; 104: 1450-1458.
- [38] Whitnall M, Howard J, Ponka P and Richardson DR. A class of iron chelators with a wide spectrum of potent antitumor activity that overcomes resistance to chemotherapeutics. *Proc Natl Acad Sci U S A* 2006; 103: 14901-14906.
- [39] Yuan J, Lovejoy DB and Richardson DR. Novel di-2-pyridyl-derived iron chelators with marked and selective antitumor activity: in vitro and in vivo assessment. *Blood* 2004; 104: 1450-1458.
- [40] Jansson PJ, Yamagishi T, Arvind A, Seebacher N, Gutierrez E, Stacy A, Maleki S, Sharp D, Sahni S and Richardson DR. Di-2-pyridylketone 4,4-Dimethyl-3-thiosemicarbazone (Dp44mT) overcomes multidrug resistance by a novel mechanism involving the hijacking of lysosomal p-glycoprotein (Pgp). *J Biol Chem* 2015; 290: 9588-9603.
- [41] Marino G, Niso-Santano M, Baehrecke EH and Kroemer G. Self-consumption: the interplay of autophagy and apoptosis. *Nat Rev Mol Cell Biol* 2014; 15: 81-94.
- [42] Eisenberg-Lerner A, Bialik S, Simon HU and Kimchi A. Life and death partners: apoptosis, autophagy and the cross-talk between them. *Cell Death Differ* 2009; 16: 966-975.
- [43] Wong VK, Li T, Law BY, Ma ED, Yip NC, Michelangeli F, Law CK, Zhang MM, Lam KY, Chan PL and Liu L. Saikosaponin-d, a novel SERCA inhibitor, induces autophagic cell death in apoptosis-defective cells. *Cell Death Dis* 2013; 4: e720.
- [44] Voss V, Senft C, Lang V, Ronellenfitsch MW, Steinbach JP, Seifert V and Kogel D. The pan-Bcl-2 inhibitor (-)-gossypol triggers autophagic cell death in malignant glioma. *Mol Cancer Res* 2010; 8: 1002-1016.
- [45] Sahni S, Bae DH, Lane DJ, Kovacevic Z, Kalinowski DS, Jansson PJ and Richardson DR.

## Dp44mT suppresses osteosarcoma

- The metastasis suppressor, N-myc downstream-regulated gene 1 (NDRG1), inhibits stress-induced autophagy in cancer cells. *J Biol Chem* 2014; 289: 9692-9709.
- [46] Scherz-Shouval R, Shvets E, Fass E, Shorer H, Gil L and Elazar Z. Reactive oxygen species are essential for autophagy and specifically regulate the activity of Atg4. *EMBO J* 2007; 26: 1749-1760.
- [47] Kurz T, Gustafsson B and Brunk UT. Intralysosomal iron chelation protects against oxidative stress-induced cellular damage. *FEBS J* 2006; 273: 3106-3117.
- [48] Vilchez V, Turcios L, Marti F and Gedaly R. Targeting wnt/beta-catenin pathway in hepatocellular carcinoma treatment. *World J Gastroenterol* 2016; 22: 823-832.
- [49] Razzaque MS and Atfi A. TGIF function in oncogenic Wnt signaling. *Biochim Biophys Acta* 2016; 1865: 101-104.
- [50] Rennoll S and Yochum G. Regulation of MYC gene expression by aberrant Wnt/beta-catenin signaling in colorectal cancer. *World J Biol Chem* 2015; 6: 290-300.